Pergamon

Int. J. Heat Mass Transfer. Vol. 37, No. 12, pp. 1749–1758, 1994

0017-9310/94 $7.00+0.00

0017-9310(94)E0009-J

Two-phase flow regimes in narrow rectangular vertical and horizontal channels

T. WILMARTH and M. ISHII†
School of Nuclear Engineering, Purdue University, West Lafayette, IN 47907, U.S.A.

(*Received* 15 *September* 1993 *and in final form* 24 *November* 1993)

Abstract—Adiabatic concurrent vertical and horizontal two-phase flow of air and water through narrow rectangular channels, gap widths 1 and 2 mm, was investigated. This study involved the observation of flow using a charge coupled device (CCD) camera and flow regimes were determined by examining the video images. A comparison of the resulting data was made with previous experimental data and also to existing transition criteria. There were four flow regimes and three transition regions observed for vertical flow and five flow regimes and three transition regions for horizontal flow.

1. INTRODUCTION

THE STUDY of two-phase flow has predominantly consisted of flow in medium size circular tubes, $D >$ 10 mm. Recently the research has expanded to include studies in narrow rectangular channels. The behavior of a gas–liquid mixture confined to the space in narrow channels differs from that in a tube due to the increased surface forces and frictional pressure drop. This difference changes the appearance of the narrow channel flow regime map with comparison to the flow regime maps of larger rectangular channels and medium size circular tubes. It is for this reason that continued research concerning narrow channel flow regimes is necessary. The need for studying small rectangular channels is abundant, as there are many applications in which two-phase flow through narrow passages is encountered. In the field of microelectronics, narrow channels are employed in the cooling systems. In the case of nuclear engineering, this type of flow is encountered in high conversion nuclear reactors, liquid metal cooled reactors and high flux research reactors. For instance, in high conversion pressurized water reactors, distances between rods in fuel bundles can be as narrow as 1 mm. A clear understanding of the flow in narrow rectangular channels is also an integral part of the design of compact heat exchangers in boiling or condensation in space, aircraft and other applications. It is this primary need for further analysis of two-phase flow in narrow rectangular channels that warrants more investigation concerning flow regime pattern identification, transition criteria, void fraction and interfacial area concentration.

This study addresses the characterization of two-phase flow in narrow rectangular channels using flow regime maps. Two test sections have been examined with gap widths of 1 and 2 mm with channel widths of 20 and 15 mm, respectively. The 1 mm gap width test section was investigated in vertical flow and the 2 mm gap width test section in vertical and horizontal flow with the longer side vertical. Comparisons of the data obtained in this study with existing data for similar flow conditions and traditional two-phase flow regime transition models are made.

2. LITERATURE REVIEW OF SMALL FLOW SYSTEMS

This section discusses the publications on two-phase flow in rectangular channels with gap width smaller than 7 mm. This review indicates that some work has been carried out in this area, however, quite inconsistent results and conclusions have been made by various researchers. Some confusion may stem from the variety of distinctions used in defining the flow regime transitions or the flow patterns themselves. Considering the flow regime map, it is commonly accepted that it be constructed using dimensional coordinates such as superficial gas and liquid velocities to describe two-phase flow [1–11], or non-dimensional parameters [12–16].

Sadatomi *et al.* [2] conducted experiments using vertical channels of different geometries. The seven two-phase channels consisted of four rectangular channels, one isosceles, one concentric annulus and one circular test section. Both two-phase and single-phase flow were considered in the noncircular channels. The friction factor was correlated using Reynolds number using the turbulent geometry factor and was described empirically as a function of the laminar

† To whom correspondence should be addressed.

NOMENCLATURE

a_i	interfacial area concentration [m^{-1}]
A	reference area [m^2]
C_1	laminar geometry factor
C_0	distribution parameter given by equation (5)
D	reference diameter [m]
D_h	hydraulic diameter given by equation (3) [m]
g	gravitational constant [m s^{-2}]
G	gap width [m]
h_g	height of gas phase given by equation (10) [m]
H	distance between pressure taps [m]
j_g, j_f	superficial velocity of gas and liquid [m s^{-1}]
l_E	entry length [m]
L	test section length [m]
p	perimeter [m]
Q_g, Q_f	volumetric flow rate of gas and liquid [m^3 s^{-1}]
V	window viewing length [m]
W	test section width [m].

Greek symbols

α	void fraction of gas phase
ρ_g, ρ_f	density of gas and liquid [kg m^{-3}]
σ	surface tension [N m^{-1}].

Subscripts

g	gas phase
f	liquid phase
O	reference.

geometry factor, C_1, of the channel considered. For the two-phase friction multiplier, the correlation proposed by Chisholm and Laird [17] was applied. The coefficient, C_1, was found to be almost equal to the ratio of the maximum to mean velocity of the cross section and the bubble rise velocity in a still water column. The mean void fraction data were related using the equation used by Griffith and Wallis [14] and Nicklin *et al.* [18]. This method agreed well for void fraction less than 0.8. It was also found that the channel geometry had no significant influence on flow transitions from bubbly to slug flow and from slug to annular for hydraulic diameter, $D_h = 4A/p \geqslant 10$ mm.

Lowry and Kawaji [5] performed an experiment in narrow vertical flow channels and found significant differences between flow in small channels to those larger than 10 mm. They determined that the existing predictions of flow transitions were inadequate to be used for the narrow rectangular channels and they developed a predictive model for the slug/churn to annular transition based upon the break up of liquid bridges. It was reported that this model compared well with the experimental results. It was also found that the two-phase friction multiplier depended on the superficial gas velocity but not on either liquid superficial velocity or gap width.

Mishima *et al.* [6] used image processing techniques to study flow in narrow rectangular ducts using either optical methods or neutron radiography technique. They obtained data for void fraction, α, and interfacial area concentration, a_i, using image processing and compared the results for void fraction with conductance probe measurements. The results of both techniques were consistent when compared. The interfacial area concentration data showed a strong correlation to the void fraction data. Flow regime maps were also obtained in this study for slug, churn and annular regimes.

Osakabe *et al.* [7] modelled the annular flow transition in narrow rectangular channels in addition to defining and proposing a model for the transition void fraction. The correlation was derived from the liquid and gas momentum equations using the Wallis shear stress correlations [19]. This transition model agreed well with the experimental data. They also found that, as the gap width became smaller, the superficial gas velocity was smaller for the annular transition.

Wambsganss *et al.* [8] examined two-phase flow patterns and frictional pressure gradients in small rectangular channels. In comparison with other work done in small circular channels, they found that the maps were not similar and could not be used as a quantitative basis. A correlation was developed for the frictional pressure gradient after it was found that the existing correlations would not be sufficient to predict the data. Finally, prediction methods for flow transitions were examined extensively.

Ali and Kawaji [9] analyzed flow in narrow rectangular channels for horizontal and vertical orientations. Flow regime maps were produced and the two-phase friction factor was correlated with void fraction using the Martinelli correlation. They found the correlation agreed well with the experimental data. The data for the flow regime maps were found using a probability density function (PDF) plotting method and neutron radiography. Pressure drop was measured, and local cross section averaged void fraction data was found using a dual system of probes and electrodes comparing the electrical conductivity of the air–water mixture to that of simply water.

Ali *et al.* [10] supplemented the previous work [9] by extending the experiment to include a test section of smaller gap width and rotating the test section including angled data as well. They produced flow maps and Martinelli correlated frictional pressure data.

Mishima *et al.* [11] used the same experimental apparatus as described previously [6] to produce flow regime maps for the three different test sections. Void fraction was measured using the neutron radiography technique and correlated with the drift flux model. The void fraction data were determined to agree well with this correlation. The average slug bubble velocity was correlated using the drift flux model and the distribution parameter was found to be smaller than usual. They also found that the shape and motion of the gas phase in a narrow channel were strongly restricted due to the proximity of the walls. Finally, the pressure data were correlated using the Chisholm–Laird [17] correlation and agreed well. It was noted that the Chisholm parameter decreased from 20 to zero as the gap width decreased from 5 to 1 mm.

Troniewski and Ulbrich [12] investigated both vertical and horizontal flow in rectangular channels to determine flow regime maps and to develop a method for calculating pressure drop in a two-phase mixture. The conclusions made use of a correction factor, which was a function of geometry derived from the analysis of single phase flow through rectangular channels. Thus, a modified Lockhart–Martinelli method was used for the pressure drop of two-phase flow through rectangular channels.

Petrick [20] studied two-phase flow in vertical rectangular channels with aspect ratios varying from 2 to 16. It was found that the fluid densities changed during both types of area changes tested (contraction and expansion) but the magnitude of change was small and could be predicted using a semi-theoretical equation. The effect of changing the mass flow rate showed a marked change in the two-phase friction factor multiplier, which was not accounted for in the Martinelli correlation. Finally, a method for measuring the void fraction was developed using a traversing technique that provided a continuous trace of the phase distribution using radiation attenuation. This method showed good agreement when compared to existing data.

Sato *et al.* [21] examined two-dimensional, two-phase flow in a vertical annulus with a small gap width. Using image processing and by adding a black dye to the liquid, they were able to determine the void fraction.

Ide and Matsumura [22] studied the effects of aspect ratio, hydraulic diameter and angle of inclination on the two-phase pressure drop. The test section consisted of a rectangular channel and the experimental results were compared with both the Lockhart–Martinelli and Akagawa correlations. It was found that the experimental data did not agree well with these correlations for large inclination angles and small superficial liquid velocities. An attempt was made to relate the pressure drop behavior to the change in flow regime using a correlation developed from a separated flow model. This correlation found good agreement with experimental results.

3. EXPERIMENTAL APPARATUS

A schematic diagram of the test loop is shown in Fig. 1(a). The water was supplied by a pump and was regulated by rotameters. The water flow entered on both sides of the cylindrical lower plenum of the test section and exited into the upper plenum where the two-phase flow was separated. The water was then drained to a collection tank to be recirculated through the system. The air flow was provided by a compressed air supply and was also controlled with rotameters. The air was then injected into the lower plenum by a 2.0 micron porous tube. This bubble generator produced uniformly sized bubbles in the mixing chamber,

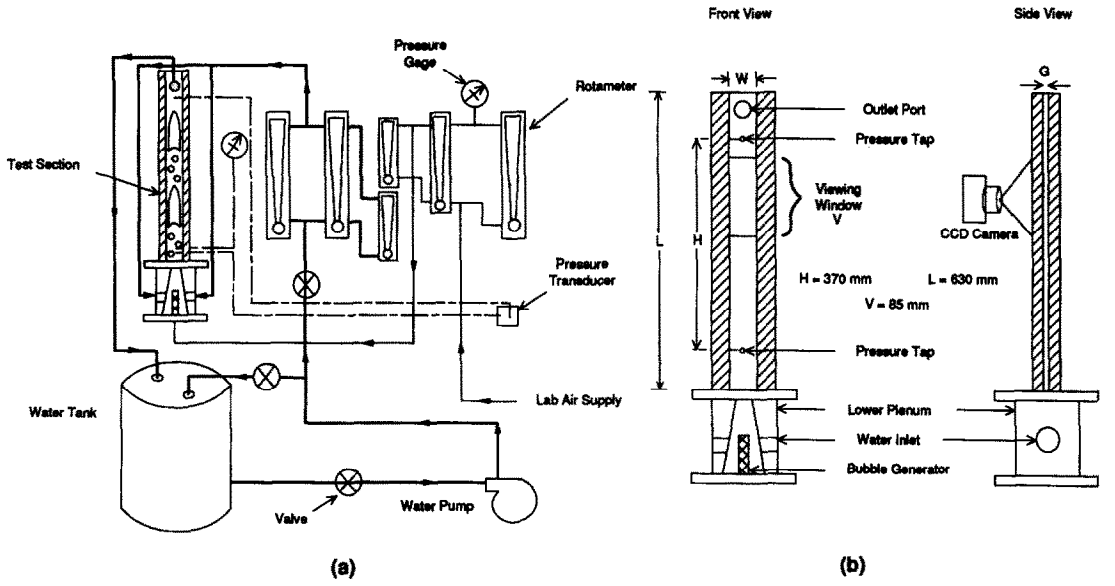

FIG. 1. (a) Schematic of vertical air–water two-phase flow loop. (b) Design of test section in vertical orientation.

which then mixed with the water before entering the test section. The test section schematic is shown in Fig. 1(b). The two flat plates were made of clear Lucite and connected with bolts. The gap was formed by sealing two stainless steel strips between the plates. The test section was 630 mm in length with two pressure taps separated by 370 mm, one located 130 mm beyond the entrance and one 130 mm before the exit of the test section. The pressure taps were connected to a pressure transducer for pressure drop measurements.

The two test sections used in this experiment were made with slightly differing dimensions: the gaps were 1 and 2 mm with channel widths 20 and 15 mm, respectively. The same overall structure was used for the 1 and 2 mm gap widths by simply replacing the highly polished stainless steel strips. The 2 mm test section was rotated 90 degrees for the horizontal flow experiment as well, with the long side vertical. Depending on the gas and liquid rates, different flow regimes were established in the test section. Measurements included pressure drop data and local average liquid and gas flow rates. A visualization study was performed to determine the flow regimes by videotaping the flow with a charge coupled device (CCD) camera. Lighting was adjusted carefully to assure high contrast for easy identification of the air–water interface. A shutter speed of 1/10 000 s was used for clarity. The window length was 85 mm and was located 380 mm beyond the entrance to yield fully developed flow. The images acquired by the camera were then digitized for analysis by an image processing system. Sample digitized images for each type of flow encountered are illustrated in Fig. 2 for vertical flow and Fig. 3 for horizontal flow.

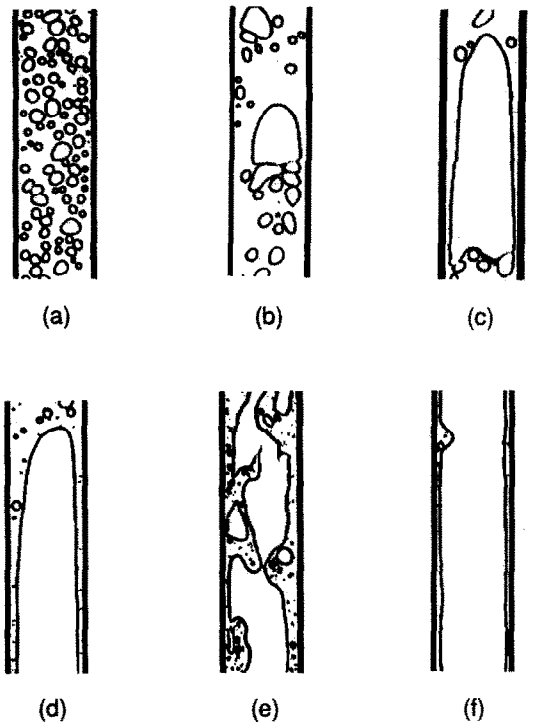

FIG. 2. Sample digitized images of vertical flow regimes: (a) bubbly flow, (b) cap–bubbly flow, (c) slug flow, (d) slug–churn transition, (e) churn-turbulent flow and (f) annular flow.

4. EXPERIMENTAL RESULTS AND DISCUSSION

4.1. *Flow regimes*

In the narrow channel flow, four regimes were recognized and three transition regions were recorded for vertical flow. The flow regimes consisted of bubbly, slug, churn-turbulent and annular flow while the transition regions were cap–bubbly, elongated slug flow, while a churn-turbulent to annular region was also recognized but not recorded on the flow pattern maps. The classification of these flows was made based on the following characterization.

Bubbly Flow—this flow was characterized by a distribution of small discrete bubbles, reasonably uniform in the axial direction in a continuous flowing liquid phase.

Cap–Bubbly Transition—as the gas flow rate increased, the confinement of the walls caused the growing bubbles to be flattened and distorted to appear as small caps. It was often characterized by coalescence of the bubbles into larger caps with width up to 60% of the channel width.

Slug Flow—this flow had large 'Taylor bubbles' which were separated by liquid slugs that bridge the test section and often carried small bubbles. The width of the gas slugs spanned more than 75% of the test section width.

Slug–Churn Transition—as the individual slug bubbles began to interact with one another, the preceding wake deformed the smooth interface of the following slugs. This caused a churn type action to begin but the individual slugs could still be identified.

Churn-Turbulent Flow—this flow was similar to slug flow but was much more chaotic, frothy and disordered. The bullet shaped slug bubbles were narrower and distorted until they were no longer discernible. The continuity of the liquid bridges was repeatedly destroyed due to the high local gas concentration in the liquid slug. Typical of churn flow was the oscillatory or alternating direction of the motion of the liquid.

Churn–Annular Transition—once the liquid bridges collapsed, there were only 'fingers' of liquid remaining between the gas and liquid phases. These fingers could reach across the width of the test section, but did not form a complete bridge as in the case of slug flow.

Annular Flow—this flow was comprised of a solid gaseous core, continuous in the axial direction, with a liquid film surrounding the core.

For the horizontal configuration, the observed flows were stratified smooth, plug, slug, dispersed bubbly and wavy annular. The transition regions con-

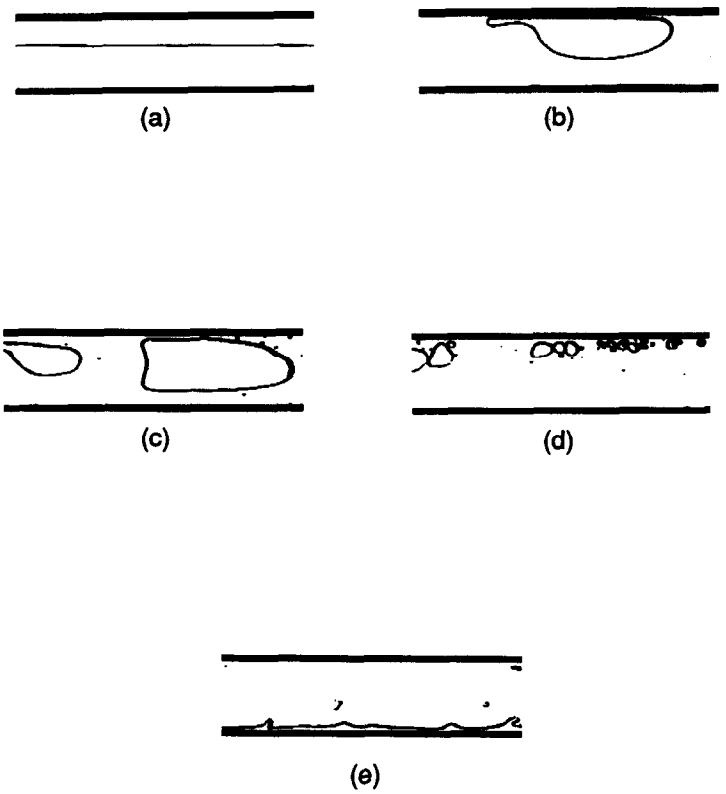

FIG. 3. Sample digitized images of horizontal flow regimes: (a) stratified smooth flow, (b) plug flow, (c) slug flow, (d) dispersed bubbly flow and (e) wavy annular flow.

sisted of elongated plug, elongated slug (churn-turbulent) and cap–bubbly. These flows were characterized by the following descriptions.

Stratified Smooth Flow—liquid flowed along the bottom of the test section with a continuous gas flow along the top. It should be noted that in this narrow channel experiment there was no stratified wavy regime observed.

Elongated Plug Transition—as the liquid flow increased, the liquid formed a bridge across the channel. The bubbles formed by this action were very smooth plugs of gas moving along the top part of the test section. The liquid bridges formed in a non-uniform manner in the axial direction.

Plug Flow—with greater liquid flows, the long gas slugs became smaller and appeared to have a large bulb at the front of the plug and a tail at the end.

Elongated Slug Transition—with higher gas rates, the transition from stratified to slug flow had a more chaotic appearance with entrained bubbles mixed with the larger gas slugs. Unlike the plug transition, the long slugs had a rougher interface toward the end of the slug.

Slug Flow—this flow was similar to the slug flow seen in the vertical flow except that the liquid film on the bottom was slightly thicker than the film at the top of the test section.

Cap-Bubbly Transition—this transition occurred from both the plug and slug flow regimes. The larger slug and plug bubbles began to disintegrate to form small nonuniformly shaped bubbles toward the top of the test section.

Dispersed Bubbly Flow—once the slug and plug bubbles break apart, they spread further throughout the test section as the liquid rate increased. The flow is then described as dispersed bubbly. All of the larger bubbles were broken into small discrete bubbles and flowed along the top part of the test section.

Wavy Annular Flow—at very high gas velocities, $j_g \approx 15$ m s^{-1}, the stratified smooth flow no longer existed. The transition to this flow was very sudden and distinct. The liquid film at the bottom of the test section became rough and wavy, and droplets were entrained into the gaseous core. This type of flow also occurred at slightly lower gas velocities but with larger liquid velocities. In these cases, there was a film at the top of the test section as well.

These flow regimes were identified by observing the video images obtained from the CCD camera. The images were then digitized for further analysis and some examples of these are shown in Fig. 2 for the vertical flow and Fig. 3 for horizontal flow.

These experimental data were then represented in flow regime maps where the parameters superficial liquid velocity, $j_f = Q_f/A$, versus the superficial gas velocity, $j_g = Q_g/A$, were used. These plots are shown in Fig. 4(a) for the 1 mm gap width test section, Fig.

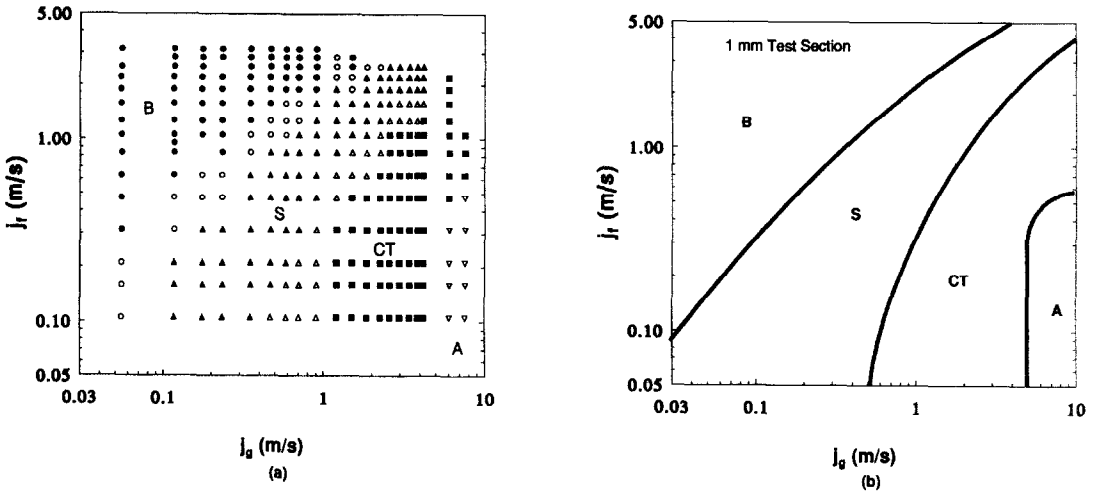

FIG. 4. (a) Flow regime map for 1 mm vertical test section. (b) Transition lines for 1 mm vertical test section. B—bubbly, S—slug, CT—churn-turbulent and A—annular.

5(a) for the vertical 2 mm test section and Fig. 6(a) for the horizontal 2 mm test section. For the horizontal test section, the transition regions were combined with the major flow regimes to simplify the map. Specifically, the transition to bubbly flow was included in the bubbly flow and the elongated plug and slug regions were included in the plug and slug regimes, respectively. The actual transition regions for the vertical flow were wide bands between each of the flow regimes: however, they were represented by single lines in Fig. 4(b) for the 1 mm gap width test section, Fig. 5(b) for the vertical 2 mm test section and Fig. 6(b) for the horizontal 2 mm test section. Because of the wide band of transition, the location of the transition line represented the general trends and may not be determined precisely.

4.2. *Comparison to existing data*

The flow regime maps obtained from this experiment were compared to existing data for air–water flow at similar conditions. Figure 7(a) shows the comparison of the vertical 1 mm test section data compared with data from Ali and Kawaji [9]. The transitions were similar for bubbly and annular flow; however, the slug and churn regimes were somewhat different. This was explained by the differences in flow geometry since the widths were a factor of four different. In comparison to a test section that was much closer in geometry, Fig. 7(b) shows the transitions of Mishima *et al.* [11]. This test section was only a factor of two different for the test section width and the data agrees well for the bubbly to slug transition. A significant difference was that no churn-turbulent flow regime was noted for the Mishima *et al.* experiment. Figure 8(a) shows the comparison of the 2 mm vertical test section with data of Lowry and Kawaji [5]. In this case, the slug to churn turbulent transition agreed well with only a discrepancy concerning the bubbly to slug transition. In Fig. 8(b) the data of Mishima *et al.* [11] agreed very well with the present work for all regime

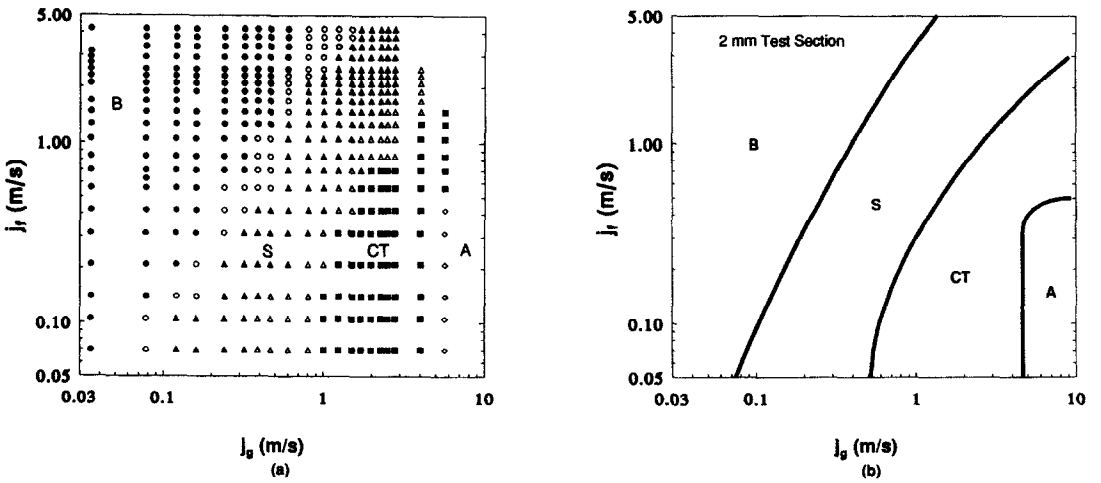

FIG. 5. (a) Flow regime map for 2 mm vertical test section. (b) Transition lines for 2 mm vertical test section. B—bubbly, S—slug, CT—churn-turbulent and A—annular.

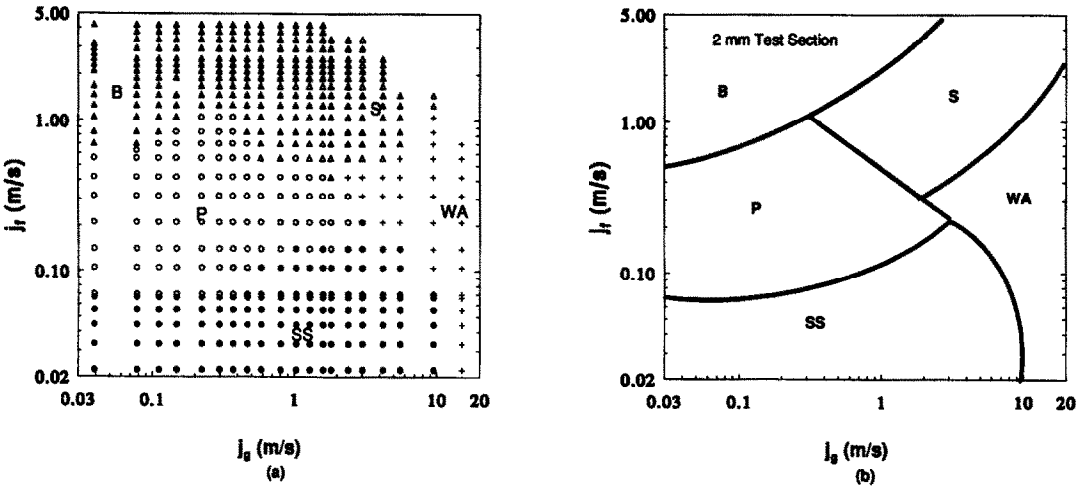

FIG. 6. (a) Flow regime map for 2 mm horizontal test section. (b) Transition lines for 2 mm horizontal test section. SS—stratified smooth, P—plug, S—slug, B—bubbly, WA—wavy annular.

transitions except some difference for the annular transition. Figure 9(a) gives the comparison for the horizontal test section and work done by Wambsganss *et al.* [8] and Fig. 9(b) shows Ali *et al.* [10] flow transitions.

4.3. *Comparison with existing transition correlations*

Applying the traditional two-phase flow regime transition criteria based on the gas and liquid superficial velocities, a comparison was made between the experimental data and two different models, one proposed by Taitel *et al.* [1] and the other by Mishima and Ishii [4].

For vertical flow, Taitel *et al.* [1] developed their model based on the physical mechanisms depending on the type of transition. The bubbly–slug transition considered the maximum allowed packing of the bubbles. The developed equation characterized this transition for conditions that do not have dispersion forces dominating. This equation is given by:

$$j_f = 3.0j_g - 1.15\left(\frac{g\Delta\rho\sigma}{\rho_f^2}\right)^{0.75}. \quad (1)$$

Where $\Delta\rho = \rho_f - \rho_g$, j_f is the superficial liquid velocity and j_g is the superficial gas velocity. For the slug to churn-turbulent transition, the mechanism was based on the characterization of flow when oscillatory motion of the liquid begins. This was expressed by:

$$\frac{l_E}{D} = 40.6\left(\frac{j_g + j_f}{\sqrt{(gD)}} + 0.22\right), \quad (2)$$

where l_E/D is the dimensionless entry length for churning and D is the hydraulic diameter:

$$D_h = 4\frac{A}{p} \quad (3)$$

where p is the perimeter. Comparisons of these equations to experimental data are shown in Fig. 10 for the 1 mm gap width test section and Fig. 11 for the

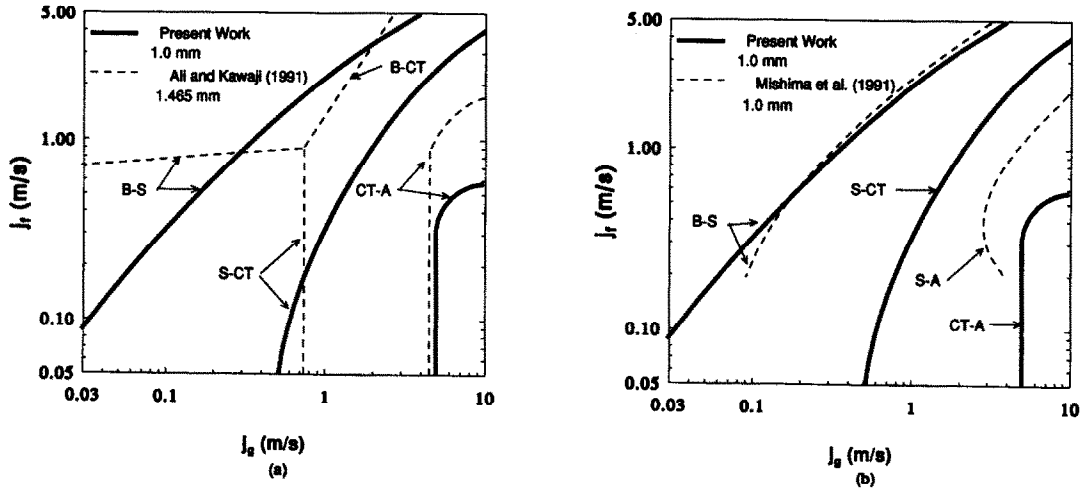

FIG. 7. Flow regime map for 1 mm gap vertical flow comparison with (a) Ali and Kawaji [9] and (b) Mishima *et al.* [11].

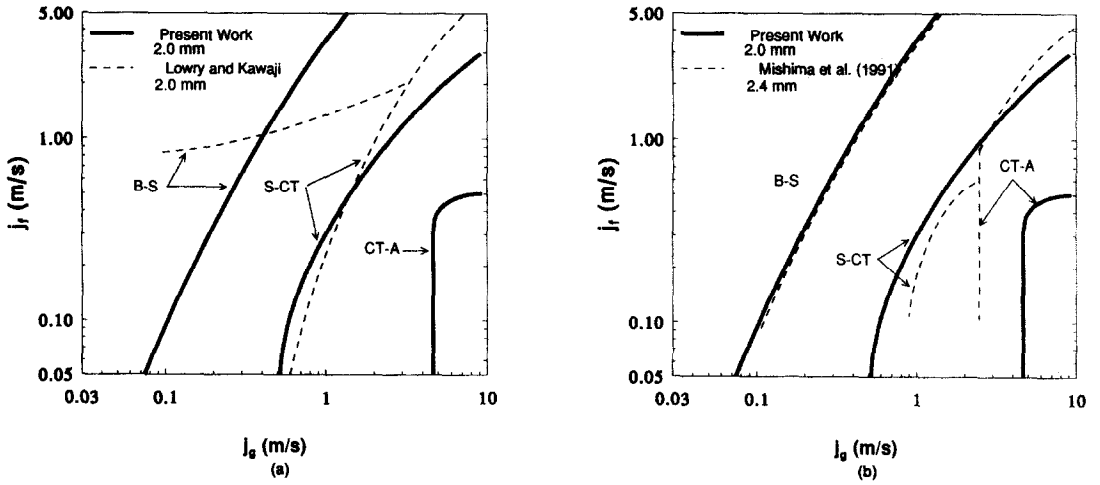

FIG. 8. Flow regime map for 2 mm gap vertical flow comparison with (a) Lowry and Kawaji [5] and (b) Mishima *et al.* [11].

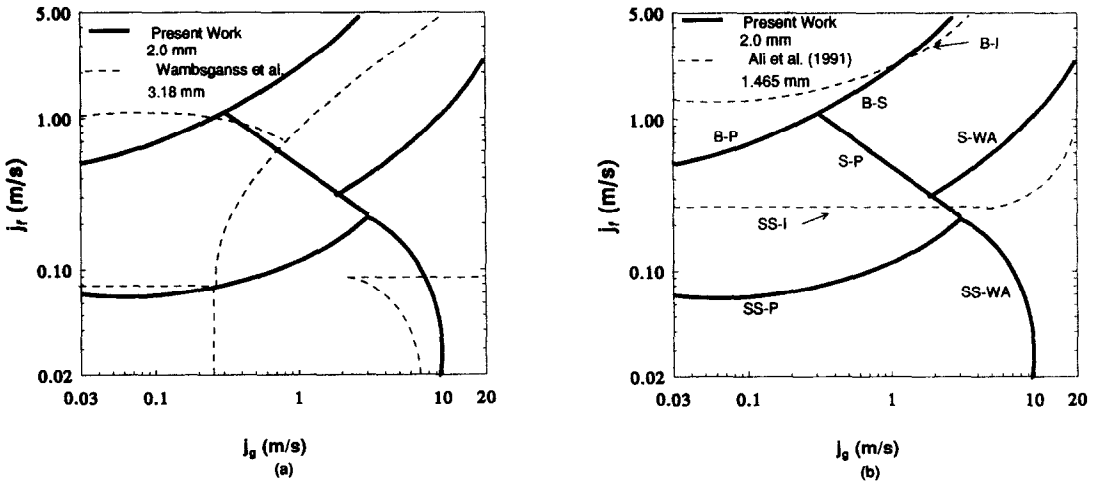

FIG. 9. Flow regime map for 2 mm gap horizontal flow comparison with (a) Wambsganss *et al.* [8] and (b) Ali *et al.* [10]. I—intermittent.

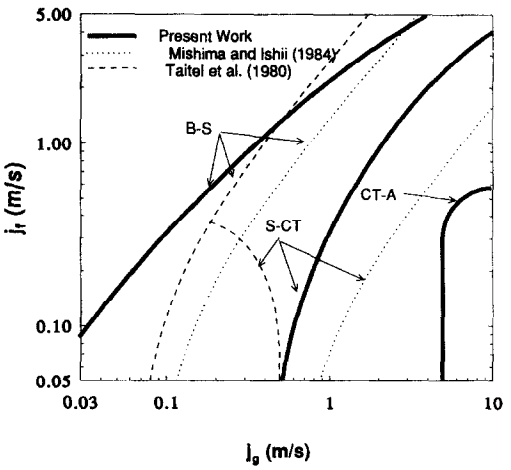

FIG. 10. Flow regime transition comparison with theory for 1 mm gap vertical flow.

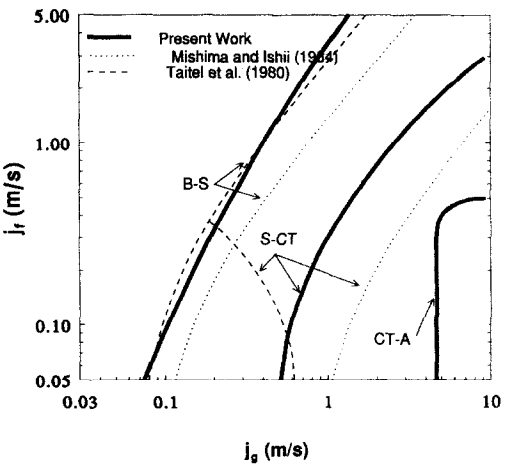

FIG. 11. Flow regime transition comparison with theory for 2 mm gap vertical flow.

2 mm gap width test section. The 1 mm gap data adequately agree for the bubbly–slug transition since the general trend is recognizable. As seen in Fig. 4(a), the theoretical transition line falls within the band of the cap–bubbly transition region. The 2 mm test section transition agrees very well with the theoretical transition line as seen in Fig. 11. For the slug to churn-turbulent theoretical transition line, the experimental data do not agree for either of the test sections.

Mishima and Ishii [4] modelled the vertical flow bubbly–slug transition using simple geometrical considerations to obtain $\alpha = 0.3$ for the criterion. Then applying the drift flux model [23] for the relationship between the superficial gas and liquid velocities, the transition criterion becomes:

$$j_f = \left(\frac{3.33}{C_0} - 1\right) j_g - \frac{0.76}{C_0}\left(\frac{\sigma \Delta \rho g}{\rho_f^2}\right)^{1/4}, \tag{4}$$

where C_0 is the distribution parameter given by:

$$C_0 = 1.35 - 0.35\sqrt{\left(\frac{\rho_g}{\rho_f}\right)} \tag{5}$$

for rectangular ducts. The slug–churn transition used the criterion that the mean void fraction be greater than the slug–bubble section mean void fraction, thus:

$$\alpha \geqslant 1 - 0.813 \times \left(\frac{(C_0 - 1) + 0.35\sqrt{(\Delta \rho g D/\rho_f)}}{j_g + j_f + 0.75\sqrt{(\Delta \rho g D/\rho_f)}(\Delta \rho g D^3/\rho_f v_f^2)^{1/18}}\right)^{0.75}. \tag{6}$$

For weakly viscous fluids, such as water, the term raised to the 1/18 power can be approximated by:

$$\left(\frac{\Delta \rho g D^3}{\rho_f v_f^2}\right)^{1/18} \approx 3, \tag{7}$$

and, to compare with experimental data, equation (6) is equated to the relationship for the void fraction based on the drift flux model [23]:

$$\alpha = \frac{j_g}{C_0(j_g + j_f) + 0.35\sqrt{(\Delta \rho g D/\rho_f)}}, \tag{8}$$

where C_0 is found from equation (5) and D is taken as the hydraulic diameter given by equation (3). Finally, the churn–annular transition was found based on the mechanism of flow reversal of the liquid film surrounding the large slug bubbles. This used the annular drift-velocity correlation [23] with $j_f = 0$ and then approximated by:

$$j_g = (\alpha - 0.11)\sqrt{\left(\frac{\Delta \rho g D}{\rho_g}\right)}, \tag{9}$$

where α is given by equation (8). Comparing these correlations with experimental data, Fig. 10 shows the results for the 1 mm gap width test section and Fig. 11 shows the results for the 2 mm gap width test section. In each case, they agree sufficiently for each transition within the transition bands of Fig. 4(a) and Fig. 5(a). The discrepancies could be accounted for by the value used for C_0. For smaller gap widths, it has been observed that the distribution parameter becomes smaller, $C_0 \sim 1.0$–1.1 [11, 24]. This would cause the theoretical transition lines to shift slightly to the left which would better agree with experimental data. On the other hand, it has also been reported that values larger than 1.3 exist for the distribution parameter for the smaller test sections [25].

For horizontal flow, the modified model of Barnea *et al.* [3] was used in the transition from stratified smooth to slug flow. This model takes into account the surface tension forces at low gas and liquid flow rates by comparing the gravity and surface forces. This equation represents the onset of intermittent or slug/plug flow:

$$h_g \leqslant \frac{\pi}{4}\sqrt{\left(\frac{\sigma}{\rho g[1 - (\pi/4)]}\right)}, \tag{10}$$

where h_g is the gas phase height. To apply this equation to experimental data, the momentum equation for each phase is solved in order to relate h_g as a function of j_g and j_f. Assuming equilibrium stratified flow, equating the pressure drop of both phases in the momentum balance, and applying the laminar friction factor for the shear stresses, the equation is found for this relation. The result of this theory is shown in Fig. 12 for the transition from stratified smooth to plug (intermittent) flow. The theoretical transition line is valid only for the stratified smooth to plug transition, such as for small gas velocities, but the line seems to better agree with the annular wavy to slug transition. The theory is not accurate since it does not take into account the increased friction caused by the narrow aspect of the test section. Thus, a better model is needed which describes this type of transitional phase including the loss due to friction.

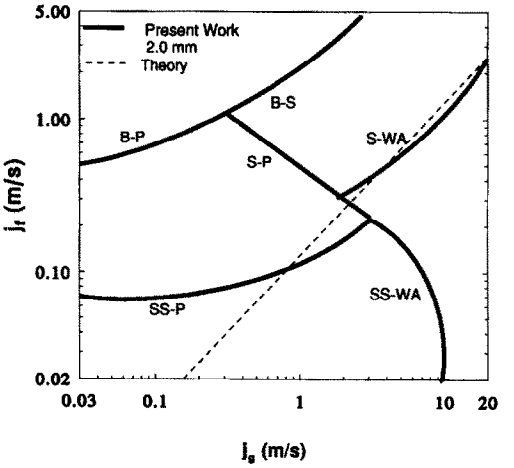

FIG. 12. Flow regime transition comparison with theory for 2 mm gap horizontal flow.

5. SUMMARY AND CONCLUSIONS

A study of two-phase flow regimes in narrow rectangular channels has been performed. The resulting data have been compared to previous experimental data [5, 8–11] and also to existing transition criteria [1, 3, 4]. A more detailed description of the flow regimes is also provided for future comparison to data concerning flow regime transitions.

The comparison to transition criteria developed by Mishima and Ishii [4] showed good agreement for vertical flow in both channels for the bubbly to slug transition, equation (4), but a new model is needed for the prediction of the distribution parameter, C_0, for narrow rectangular channels. For the slug to churn-turbulent transition given by equations (6) and (8), the results were less satisfactory, also due to the model of the distribution parameter, C_0. Finally, the annular transition given by equations (8) and (9), showed good agreement with experimental data for both vertical test sections. In these channels, the transition was caused by the droplet entrainment process. Thus the transition criterion [4] based on this mechanism indicated that the entrainment phenomena were well scaled by the criterion.

The Taitel *et al.* [1] transition model for bubbly to slug flow, equation (1), agreed adequately for both the vertical test sections. The slug to churn-turbulent transition given by equation (2), however, did not provide a good comparison to the experimental data.

For horizontal flow, the model for transition applied was found to be unsatisfactory in predicting the transition from stratified smooth to plug flow. This model was shown in equation (10) applied to experimental data with the momentum balance of each phase.

Future work in this area consists of two-phase pressure drop data and void fraction and interfacial area concentration data for narrow channel flow which will be correlated using a drift flux correlation.

Acknowledgements—This work was performed under the auspice of the U.S. Department of Energy, Office of Basic Energy Science. The authors would like to express their appreciation for the encouragement, support and technical advice on this work from Dr O. P. Manley. Appreciation for technical advice is also expressed to Dr S. T. Revankar and colleagues of the School of Nuclear Engineering Thermal-hydraulics and Reactor Safety Lab of Purdue University.

REFERENCES

1. Y. Taitel, D. Bornea and A. E. Dukler, Modelling flow pattern transitions for steady upward gas–liquid flow in vertical tubes, *A.I.Ch.E. Jl* **26**(3), 345–354 (1980).
2. M. Sadatomi, Y. Sato and S. Saruwatari, Two-phase flow in vertical noncircular channels, *Int. J. Multiphase Flow* **8**(6), 641–655 (1982).
3. D. Barnea, Y. Luninski and Y. Taitel, Flow pattern in horizontal and vertical two phase flow in small diameter pipes, *Canadian J. Chem. Engng* **61**, 617–620 (1983).
4. K. Mishima and M. Ishii, Flow regime transition criteria for upward two-phase flow in vertical tubes, *Int. J. Heat Mass Transfer* **27**, 723–737 (1984).
5. B. Lowry and M. Kawaji, Adiabatic vertical two-phase flow in narrow flow channels, *Proc. Japan–U.S. Seminar on Two-Phase Flow Dynamics*, pp. C.7-1–C.7-4 (1988).
6. K. Mishima, S. Fujine, K. Yoneda, K. Yonebayashi, K. Kanda and H. Nishihara, A study of air–water flow in a narrow rectangular duct using image processing technique, *Proc. Japan–U.S. Seminar on Two-Phase Flow Dynamics*, pp. C.3-1–C.3-12 (1988).
7. M. Osakabe, K. Tasaka and Y. Kawasaki, Annular flow transition model in channels of various shapes, *JSME, Ser. B* **54**, 953–958 (1989).
8. M. W. Wambsganss, J. A. Jendrzejczyk and D. M. France, Two-phase flow patterns and transitions in a small, horizontal, rectangular channel, *Int. J. Multiphase Flow* **17**(3), 327–342 (1991).
9. M. Ali and M. Kawaji, The effect of flow channel orientation on two-phase flow in a narrow passage between flat plates, *ASME/JSME Thermal Engng Proc.* **2**, 183–190 (1991).
10. M. Ali, M. Sadatomi, M. E. Charles and M. Kawaji, Effects of gap width and orientation on two-phase flow in a narrow passage between two flat plates, *Proc. Int. Conf. on Multiphase Flows*, pp. 15–18 (1991).
11. K. Mishima, T. Hibiki and H. Nishihara, Some characteristics of gas–liquid flow in narrow rectangular ducts, *Proc. Int. Conf. on Multiphase Flows*, pp. 485–488 (1991).
12. L. Troniewski and R. Ulbrich, Two-phase gas–liquid flow in rectangular channels, *Chem. Engng Sci.* **39**(4), 751–765 (1983).
13. O. Baker, Simultaneous flow of oil and gas, *Oil Gas J.* **53**, 185 (1954).
14. P. Griffith and G. B. Wallis, Two-phase slug flow, *ASME, Series C* **83**, 307–320 (1961).
15. E. R. Hosler, Flow patterns in high pressure two-phase (steam–water) flow with heat addition, *A.I.Ch.E. Symp. Series* **64**(82), 54–66 (1968).
16. M. Suo and P. Griffith, Two-phase flow in capillary tubes, *ASME J. Basic Engng*, 576–582 (1964).
17. D. Chisholm and A. Laird, Two-phase flow in rough tubes, *ASME* **80**, 276–286 (1958).
18. D. J. Nicklin, J. O. Wilkes and J. F. Davidson, Two-phase flow in vertical tubes, *Trans. Inst. Chem. Engrs* **40**, 61–68 (1962).
19. G. B. Wallis, *One-dimensional Two-phase Flow*, p. 322. McGraw-Hill, New York (1969).
20. M. Petrick, Two-phase air water flow phenomena, ANL Report ANL-57-87, pp. 1–88 (1958).
21. Y. Sato, M. Sadatomi, A. Kawahara and S. Asakura, An experimental method of 2-D two-phase flow (measurement of void fraction distribution using image processing), *JSME* **57**(538), 1979–1984 (1991).
22. H. Ide and H. Matsumura, Frictional pressure drops of two-phase gas–liquid flow in rectangular channels, *Exp. Thermal Fluid Sci.* **3**, 362–372 (1990).
23. M. Ishii, One-dimensional drift-flux model and constitutive equations for relative motion between phases in various two-phase flow regimes, ANL Report ANL-77-47 (1977).
24. T. Wilmarth, A study of two-phase flow characteristics in narrow rectangular channels, Master's Thesis, Purdue University School of Nuclear Engineering, IN (1993).
25. Y. Iida and K. Takahashi, Gas–liquid two-phase flow through channels with narrow spaces, *Kagaku Kogaku Ronbunshu* **2**, 228–234 (1976).